FTUAM/95-18

Approximate particle number projection for finite range density dependent forces

A. Valor, J.L. Egido, L.M. Robledo

Departamento de Física Teórica C-XI

Universidad Autónoma de Madrid, E–28049 Madrid, Spain

Abstract

The Lipkin-Nogami method is generalized to deal with finite range density dependent forces. New expressions are derived and realistic calculations with the Gogny force are performed for the nuclei ^{164}Er and ^{168}Er. The sharp phase transition predicted by the mean field approximation is washed out by the Lipkin-Nogami approach. A much better agreement with the experimental data is reached with the new approach than with the Hartree-Fock-Bogoliubov one, specially at high spins.

PACS numbers 21.60.Jz, 21.10.Ky, 21.10.Re, 27.70.+q

Mean-field theories (BCS, Hartree-Fock and Hartree-Fock-Bogoliubov, HFB) are the cornerstone of all microscopic approximations to the nuclear many body problem. The success of these approaches is mostly due to their ability to deal with single particle motion as well as with the collective motion associated with symmetries [1], the latter one by enlarging the variational Hilbert space with wave functions that are not eigenstates of the symmetry operators. These wave functions are usually constrained to accomplish the symmetries on the average; for most symmetries (with the exception of the particle number) this is a very satisfactory approach, see Ref. [1] for a thorough discussion. In the case of pairing correlations, in which we are interested in this letter, the crucial quantities are the number of correlated pairs and the level density around the Fermi surface. If these quantities are small, and in nuclei they usually are, mean field theories are not enough and one should do something better.

The ideal treatment of pairing correlations in nuclei is particle number projection before the variation [1]. At high spin this theory is rather complicated and up to now it has only been applied with separable forces [2]. On the other hand, the semi-classic recipe of solving the mean field equations with a constraint on the corresponding symmetry operator can be derived as the first order result of a full quantum-mechanical expansion (the Kamlah expansion) [3] of the projected quantities. The second order in this expansion takes into account the particle number fluctuations and might cure some of the deficiencies of the first order approximation. However, full calculations up to second order are rather cumbersome and just a simple model calculation has been carried out up to now [4]. Most second order calculations have been done using the Lipkin-Nogami (LN) recipe originally proposed in Refs. [5–7], see also the clarifying papers by Quentin et al. [8] and by Flocard at al. [4]. Recently the LN method has been applied to study superdeformed nuclei at high spins

[1] Continuous symmetries as rotations in any space: coordinate space, gauge space of particle number operator, etc, as well as with discrete symmetries, e.g. spatial parity.

adding a monopole pairing interaction to the Woods-Saxon plus Strutinsky [9] and to the Skyrme force [10].

Up to now the LN method has been only formulated for the case of a simple separable pairing interaction. The purpose of this Letter is to extend such studies to more realistic pairing interactions like the one implicit in the finite range and density dependent Gogny force where the particle-hole and particle-particle part of the interaction are generated from the same force. We have formulated the Lipkin-Nogami method using the Kamlah expansion and treated the density dependence consistently. In the new formulation additional terms arise in the equations determining the parameters of the theory.

Let $|\Phi\rangle$ be a product wave function of the Hartree-Fock-Bogoliubov type, i.e. a particle number symmetry violating wave function. We can generate an eigenstate of the particle number $|\Psi_N\rangle$ by the projection technique [1]

$$|\Psi_N\rangle = \hat{P}^N|\Phi\rangle = \frac{1}{2\pi}\int_0^{2\pi} d\phi e^{i(\hat{N}-N)\phi}|\Phi\rangle. \tag{1}$$

The particle number projected energy is given by

$$E^N_{proj} = \frac{\langle\Psi_N|\hat{H}|\Psi_N\rangle}{\langle\Psi_N|\Psi_N\rangle} = \frac{\int_0^{2\pi} d\phi e^{-i\phi N}\langle\Phi|\hat{H}e^{i\phi\hat{N}}|\Phi\rangle}{\int_0^{2\pi} d\phi e^{-i\phi N}\langle\Phi|e^{i\phi\hat{N}}|\Phi\rangle} = \frac{\int_0^{2\pi} d\phi e^{-i\phi N}h(\phi)}{\int_0^{2\pi} d\phi e^{-i\phi N}n(\phi)} \tag{2}$$

where we have introduced the hamiltonian-, $h(\phi) = \langle\Phi|\hat{H}e^{i\phi\hat{N}}|\Phi\rangle$, and norm-, $n(\phi) = \langle\Phi|e^{i\phi\hat{N}}|\Phi\rangle$, overlaps. In the case of large particle numbers and strong deformations in the gauge space associated to $\hat{N}$, one expects the $h(\phi)$ and $n(\phi)$ overlaps to be peaked at $\phi = 0$ and to be very small elsewhere in such a way that the quotient $h(\phi)/n(\phi)$ behaves smoothly. One can make an expansion of $h(\phi)$ in terms of $n(\phi)$ in the following way [3]

$$h(\phi) = \sum_{m=0}^{M} h_m\hat{\mathcal{N}}^m n(\phi) \tag{3}$$

where we have introduced the Kamlah operator $\hat{\mathcal{N}} = \frac{1}{i}\frac{\partial}{\partial\phi} - \langle\Phi|\hat{N}|\Phi\rangle$ which is a representation of the particle number operator in the space of the parameter ϕ. The expansion coefficients h_m are determined by applying the operators $1, \hat{\mathcal{N}}, ..., \hat{\mathcal{N}}^M$ on Eq. (3) and taking the limit $\phi \to 0$. From now on we shall use the shorthand notation $\langle\hat{A}\rangle = \langle\Phi|\hat{A}|\Phi\rangle$ and $\Delta\hat{N} = \hat{N} - \langle\hat{N}\rangle$.

The projected energy to second order is

$$E^{(2)}_{proj} \;=\; \langle \hat{H} \rangle \;\; - \;\; h_2 \langle (\Delta \hat{N})^2 \rangle \;\; + \;\; h_1 \, (N - \langle \hat{N} \rangle) \;\; + \;\; h_2 \, (N - \langle \hat{N} \rangle)^2, \tag{4}$$

with h_1 and h_2 given by

$$h_1 = \frac{\langle \hat{H} \Delta \hat{N} \rangle - h_2 \, \langle (\Delta \hat{N})^3 \rangle}{\langle (\Delta \hat{N})^2 \rangle} \tag{5}$$

$$h_2 = \frac{\langle (\hat{H} - \langle \hat{H} \rangle)(\Delta \hat{N})^2 \rangle - \langle \hat{H} \Delta \hat{N} \rangle \langle (\Delta \hat{N})^3 \rangle / \langle (\Delta \hat{N})^2 \rangle}{\langle (\Delta \hat{N})^4 \rangle - \langle (\Delta \hat{N})^2 \rangle^2 - \langle (\Delta \hat{N})^3 \rangle^2 / \langle (\Delta \hat{N})^2 \rangle}. \tag{6}$$

In a full variation after projection method one should vary Eq. (4). In the Lipkin-Nogami prescription, however, the coefficient h_2 is held constant during the variation; the resulting equation is much simpler, one gets

$$\frac{\delta}{\delta \Phi} \langle \hat{H} - h_2 (\Delta \hat{N})^2 \rangle - h_1 \frac{\delta}{\delta \Phi} \langle \hat{N} \rangle = 0, \tag{7}$$

with h_1 determined by the constraint

$$\langle \hat{N} \rangle = N. \tag{8}$$

If there are additional constraints, for example the angular momentum, one just has to substitute $\hat{H}$ by $\hat{H}' = \hat{H} - \omega \hat{J}_x$ in all equations above and to add the constraint $\langle \hat{J}_x \rangle = [I(I+1) - \langle \hat{J}_z{}^2 \rangle]^{1/2}$ to the one of Eq. (8).

Now we would like to generalize the formulae above to density dependent forces, like the Gogny force [11,12] which has a term proportional to $\rho^\alpha(\frac{\vec{r}_1 + \vec{r}_2}{2})$.

In this case the density term[2] causes a dependence on ϕ of the hamiltonian [13]. The Kamlah expansion (3) provides in this case the following equation system

$$\left\langle \frac{1}{i} \frac{\partial \hat{H}}{\partial \phi} \right|_{\phi=0} + \hat{H} \Delta \hat{N} \Bigg\rangle = h_1 \langle (\Delta \hat{N})^2 \rangle + h_2 \langle (\Delta \hat{N})^3 \rangle \tag{9}$$

$$\left\langle \frac{1}{i^2} \frac{\partial^2 \hat{H}}{\partial \phi^2} \right|_{\phi=0} + 2 \Delta \hat{N} \frac{1}{i} \frac{\partial \hat{H}}{\partial \phi} \Bigg|_{\phi=0} + \; \hat{H} (\Delta \hat{N})^2 \Bigg\rangle = \langle H \rangle \langle (\Delta \hat{N})^2 \rangle$$

$$+ h_1 \langle (\Delta \hat{N})^3 \rangle + h_2 \left(\langle (\Delta \hat{N})^4 \rangle - \langle (\Delta \hat{N})^2 \rangle^2 \right)$$

[2]The dependence of the density with ϕ is given by $\rho(r) = \langle \Phi | c^\dagger(r) c(r) e^{i \phi \hat{N}} | \Phi \rangle / \langle \Phi | e^{i \phi \hat{N}} | \Phi \rangle$.

which determine the coefficients h_1 and h_2.

From now on we proceed as in the non-density dependent case, i.e. we have to solve Eq. (7) with the constraint (8) but with the coefficient h_1 and h_2 provided by the equation system (9).

We have applied this formalism to study high spin states with the Gogny force in two rare earth nuclei: ^{164}Er as an example of strong back-bender and ^{168}Er as a non-back-bender. We shall refer to this calculations as cranked-HFB-LN (CHFBLN). In all our results we shall also present the ones obtained with the plain cranked HFB theory (CHFB) [14]. We are using the standard DS1 parametrization set [12]. Of course, one could ask if the parametrization of the force should be changed, for it was adjusted for plain mean field calculation. Since this is the first investigation in this direction we shall use the standard parametrization, further investigations will be reported in the future.

In Fig. 1a we show the pairing energy in the CHFB approach and in the CHFBLN approach versus the angular momentum. For ^{164}Er in the CHFB approach we observe for the neutron system, first, a strong Coriolis antipairing effect which diminishes the neutron pairing correlations, later on the crossing of the ground state band with a two neutron aligned band -see below- causes the quenching of the pairing correlations at $I \simeq 18\hbar$. The proton system, on the other hand, behaves very smoothly until $I = 18\hbar$. From $I = 18\hbar$ up to $I = 28\hbar$ we observe the typical Coriolis antipairing effect reduction, which is not as strong as for the neutron system because the intruder orbital in this case is a $h_{\frac{11}{2}}$ at variance with the $i_{\frac{13}{2}}$ of the neutrons. In the CHFBLN results the same Coriolis antipairing effects are observed but no superfluid to normal fluid phase transition is found. We also realize that the LN term has a larger effect on the proton system than on the neutron one. For ^{168}Er, Fig. 1b, again the neutron phase transition is washed out in the CHFBLN approach and a larger increase in the pairing energies of the proton system than in the neutron one is obtained; this may have to do with the different intruders for both systems.

The most relevant deformation parameters are β and γ (we define them as in Ref. [15]). Their angular momentum dependence is displayed in Figs. 1c and 1d. For ^{164}Er, in the

CHFB approach we first observe a rather constant value of the deformation parameters β until $I = 12\hbar$, from this point on and until $I = 28\hbar$ we find a decrease in β. This anti-stretching effect is caused by the Coriolis force. The CHFBLN approach differs from the CHFB one in the spin range $I = 10\hbar$ till $I = 18\hbar$, where the neutron pairing collapse take place. Along the aligned band the β values are again very similar in both approaches. In the CHFB approach, at $I = 0\hbar$ the nucleus ^{164}Er is axially symmetric ($\gamma = 0$), then γ increases up to 8 degrees at $I = 18\hbar$, later on it decreases very slowly. In the CHFBLN approach, the nucleus remains axially symmetric ($\gamma = 0$) at all spin values. In the nucleus ^{168}Er we observe a similar behavior when we compare the β-values of the CHFBLN and the CHFB at the spin range $I = 12 - 18\hbar$. From $I = 22 - 28\hbar$ we find a larger decrease in the β-values of the CHFBLN as compared with the CHFB. The reason for this behavior can be found in Fig. 3d; due to the smaller value of the moment of inertia in the CHFBLN approach as compared with the CHFB one, larger values of the cranking frequency are needed to produce the same angular momentum. These larger values of the cranking frequency causing an stronger anti-stretching effect on the β-values of the CHFBLN approach. The γ-values of ^{168}Er are close to zero in both approaches.

The $E2$ transition probabilities and the gyromagnetic factors have been calculated in the cranking approximation [14]. Since our configuration space is large enough (11 oscillator shells) no effective charges have been used in the calculations. In Fig. 2a we show the reduced transition probabilities along the Yrast band versus the angular momentum and the experimental ones for the nucleus ^{164}Er. At spin values up to $I = 10\hbar$ our theoretical results are in good agreement with the experimental data. For spin values 12, 14 and $16\hbar$, corresponding to the band crossing, we are not able to reproduce the zig-zag behavior of the experimental data. This result is not surprising since we know that the cranking approximation is not good in the band crossing. The decrease of the CHFBLN results as compared with the CHFB ones is due to the fact that in the CHFBLN approach the nucleus remain axially symmetric at this spin values while in the CHFB approach it does not. Concerning ^{168}Er, Fig. 2b, neither CHFB nor CHFBLN are able to reproduce the zig-

zag at medium spins (this behavior is not understood, to our knowledge, in any theory). The smaller values of the CHFBLN at high spins are due to the smaller β-values of this approach.

To investigate the alignment processes in these nuclei we shall study the gyromagnetic factors. In the calculation the free values of the orbital and spin gyromagnetic factors have been used and no rotor contribution g_R has been considered. In Fig. 2c we display the theoretical $g-$factors g, g_p and g_n as well as the experimental $g-$factor at $I = 2\hbar$ [18] for ^{164}Er. From the pattern of g we can conclude that at low spins we have a smooth neutron alignment, at medium spins and up to $I = 18\hbar$ we have strong neutron alignment and for higher spins we observe proton alignment. The tendency is qualitatively the same in both approximations, the CHFBLN displaying a sharper behavior though. For ^{168}Er, Fig. 2d, we obtain in the CHFB (CHFBLN) an smooth neutron alignment up to spin $16\hbar$ ($24\hbar$), later on proton alignment. The agreement with the known experimental data ($I = 6, 8$ and $10\hbar$) is excellent.

In Fig. 3a we display transition energies versus the angular momentum. For ^{164}Er the agreement with the experimental data is good at low spins in the CHFB approach while in the band crossing region we see that the crossing is not as sharp as in the experiment -this is a well known drawback of the cranking approximation. In the high spin part we get smaller values for the transition energies than in the experiment. In the CHFBLN approach at low and medium spins the agreement with the experiment is better than in the CHFB approach. In the backbending region the results are not good again, but in the very high spin region the agreement with the experiment is very good at variance with the CHFB approximation. Concerning ^{168}Er, Fig. 3b, the CHFB results are very low as compared with the experiment; the CHFBLN ones, however, are in excellent agreement with the experiment.

In Fig. 3c,d we display the moments of inertia, versus the square of the angular frequency. In ^{164}Er in the CHFBLN approach we obtain at low spins a smaller value than in the CHFB due to the larger pairing correlations in better agreement with the experiment. In the band crossing we obtain a clear back-bending although shifted in a few units as compared with

the experiment indicating, perhaps, that angular momentum projection is important in this region. For spin values $I = 18, 20, 22\hbar$, i.e. on the aligned band, the agreement with the experiment is excellent [3], at variance with the simpler CHFB approach. Concerning ^{168}Er, Fig. 3d, the results of the CHFBLN approach are much better than the ones of CHFB, we are at low spins somewhat lower than in the experiment, but at medium and high spins the agreement is very good. We would like to stress that no $\mathcal{J}_c$, the core moment of inertia, has been assumed.

In conclusion, for the first time, we have formulated the Lipkin-Nogami approximation for density dependent forces. We have performed numerical calculations with the finite range density dependent Gogny force for two nuclei, the theoretical results with this approximation are in much better agreement with the experiment than the plain HFB calculations.

This work was supported in part by DGICyT, Spain under Project PB91–0006. One of us (A.V.) would like to thank the Spanish Ministerio de Asuntos Exteriores for financial support through an ICI grant.

[3] Notice that the experimental results end at spin $I = 22\hbar$ ($I = 16\hbar$) for ^{164} Er (^{168}Er) while the theoretical ones go up to $I = 26\hbar$.

REFERENCES

[1] P. Ring and P. Shuck, *The Nuclear Many Body Problem* (1980), Springer–Verlag Edt. Berlin.

[2] J.L. Egido and P. Ring, Nucl. Phys. **A388**, 19 (1982).

[3] A. Kamlah, Z. Phys. **216**, 52 (1968).

[4] D. C. Zheng, D.W.L. Sprung and H. Flocard, Phys. Rev. bf C46, 1335 (1992).

[5] H. J. Lipkin, Ann. Phys. (N.Y.) **12**, 425 (1960).

[6] Y. Nogami, Phys. Rev. **B134**, 313 (1964); Y. Nogami and I.J. Zucker, Nucl. Phys. **60**, 203 (1964).

[7] J. F. Goodfellow and Y. Nogami, Can. J. Phys. **44**, 1321 (1966).

[8] P. Quentin, N. Redon, J. Meyer and M. Meyer, Phys. Rev. **C41**, 41 (1990).

[9] P. Magierski, S. Cwiok, J. Dobaczewski and W. Nazarewicz, Phys. Rev. **C48**, 1681 (1993).

[10] G. Gall, P. Bonche, J. Dobaczewski, H. Flocard and P.-H. Heenen, Z. Phys. **A348**, 183 (1994).

[11] D. Gogny, *Nuclear Selfconsistent fields*. Eds. G. Ripka and M. Porneuf (North Holland 1975).

[12] J.F. Berger, M. Girod and D. Gogny, Nucl. Phys. **A428**, 23c (1984).

[13] P. Bonche, J. Dobaczewski, H. Flocard, P.-H. Heenen and J. Meyer, Nucl. Phys. **A510**, 466 (1990).

[14] J. L. Egido and L. M. Robledo, Phys. Rev. Lett. **70**, 2876 (1993).

[15] M. Girod and B. Grammaticos, Phys. Rev. **C27**, 2317 (1983).

[16] S.W. Yates et al. Phys. Rev. **C21**, 2366 (1980).

[17] B. Kotlinski et al. Nucl. Phys. **A517**, 365 (1990).

[18] Nucl. Data Sheets **11**, no. 3 p. 363 (1974).

[19] F. Brandolini et al. Phys. Rev. **C45**, 1549 (1992).

FIGURES

FIG. 1. Upper panels: Pairing energies versus the angular momentum. Proton (neutron) values are represented by triangles (inverted triangles). Lower panels: Deformation parameters β (circles, scale on the left axis) and γ (squares, scale on the right axis) versus angular momentum. Full (empty) symbols correspond to CHFB (CHFBLN).

FIG. 2. Upper panels: Reduced transition probabilities $B(E2)$ (in units of $(eb)^2$) along the Yrast band as a function of the angular momentum. Full (open) circles stand for the CHFB (CHFBLN) results and full squares for the experimental data ([16] for ^{164}Er and [17] for ^{168}Er). Lower panels: Gyromagnetic factors (in units of μ_N of the Yrast states versus the angular momentum; g is represented by diamonds, g_p by circles and g_n by triangles. Full (open) symbols correspond to CHFB (CHFBLN). The experimental data ([18] for ^{164}Er and [19] for ^{168}Er) are represented by full squares.

FIG. 3. Upper panels: the gamma-ray energy $\Delta E_I = E(I) - E(I-2)$ as a function of the angular momentum. Full (open) circles stand for the CHFB (CHFBLN) results and full squares for the experimental data ([16] for ^{164}Er and [17] for ^{168}Er). Lower panels: the moment of inertia $\mathcal{J} = (2I-1)/\Delta E_I$ versus the square of the angular frequency. The meaning of the symbols is the same as in the upper panels.

Fig. 1

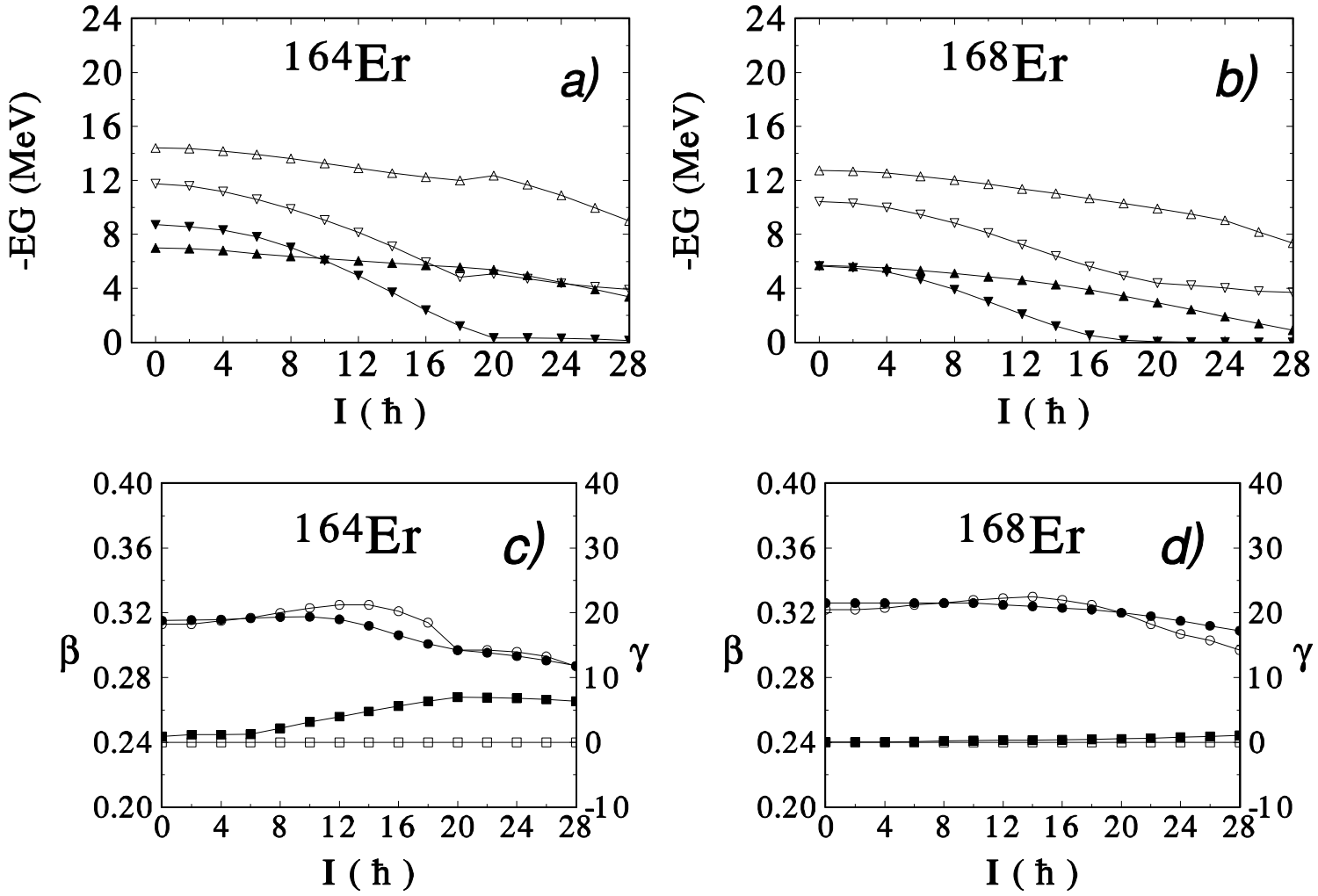

Fig. 2

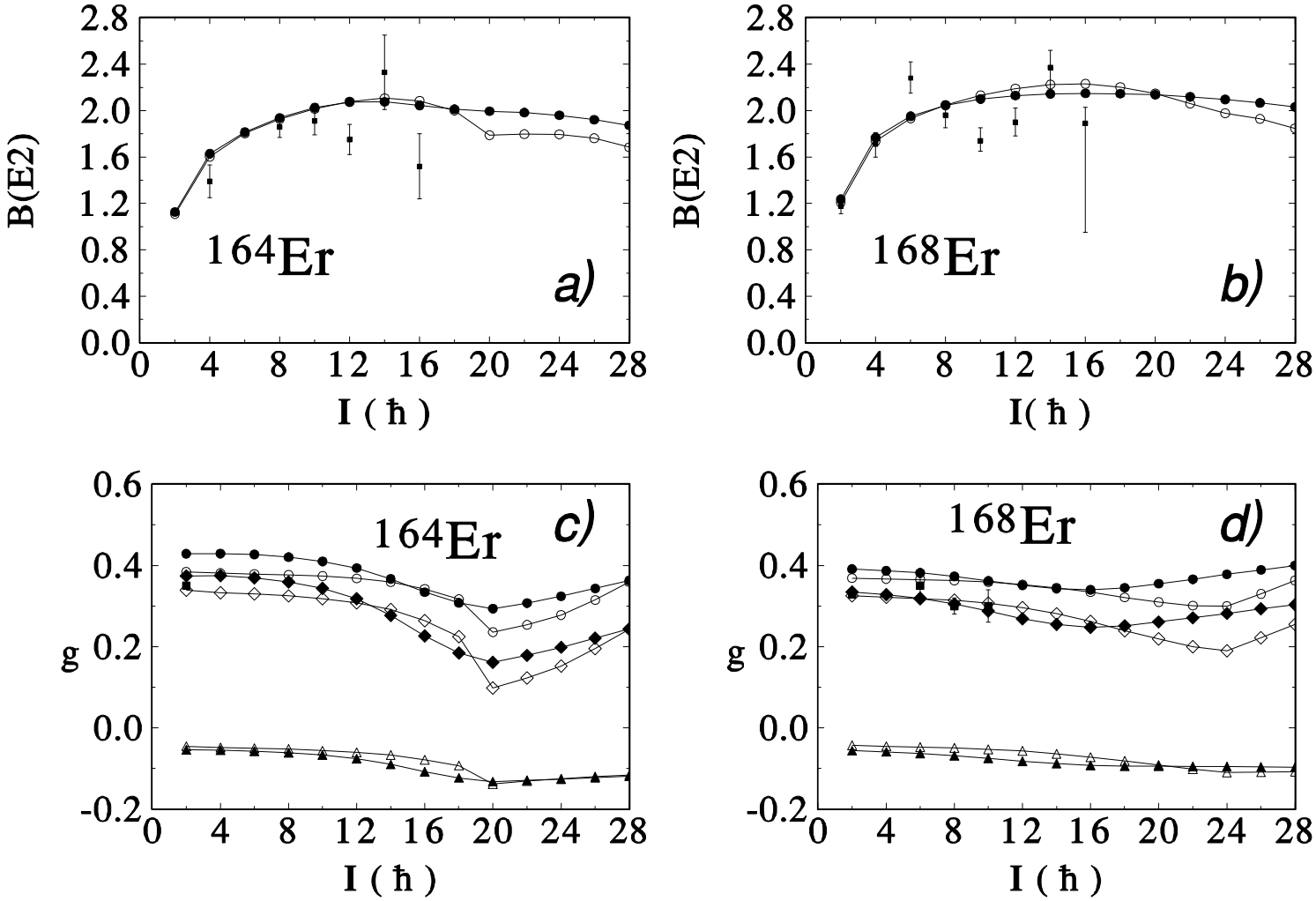
B(E2)
2.8
2.4
2.0
1.6
1.2
0.8
0.4
0.0
0
4
8
12
16
20
24
28
I (ħ)
164Er
a)
168Er
b)
I(ħ)
g
0.6
0.4
0.2
0.0
-0.2
c)
d)

Fig. 3

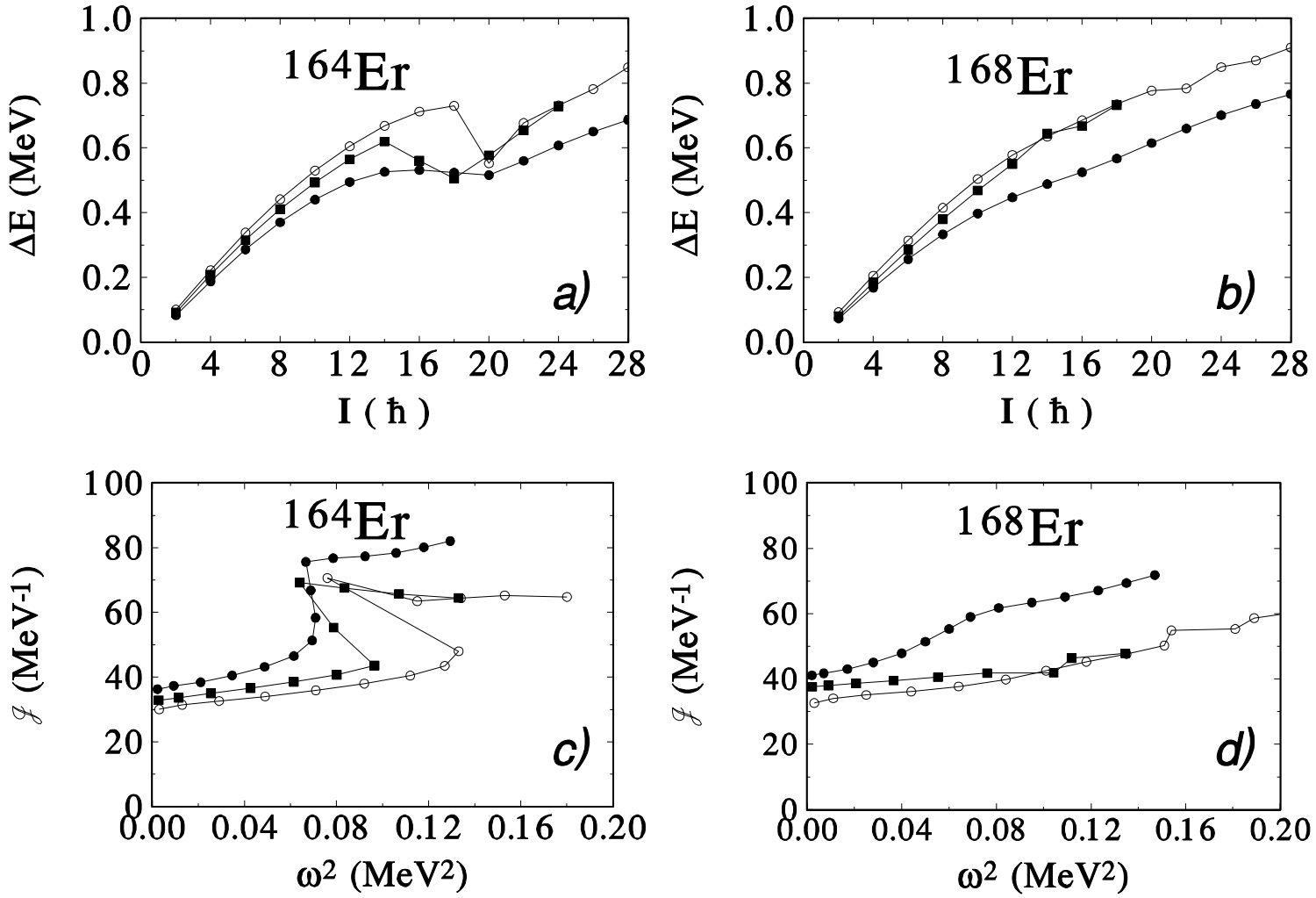
164Er
a)
ΔE (MeV)
I (ħ)
168Er
b)
ΔE (MeV)
I (ħ)
164Er
c)
ℐ (MeV-1)
ω2 (MeV2)
168Er
d)
ℐ (MeV-1)
ω2 (MeV2)